X-Ray Micro-densitometry of Amorphous MoRuB for LIGO Flex-Joint Mirror Suspensions

Eric Adam Kort
Mentor: Dr. Riccardo DeSalvo

Abstract

Suspension thermal noise has become a limitation in the resolution of the Advanced LIGO interferometer, hindering our ability to detect gravity waves at low frequency. The present baseline solution, fused silica fibers, has many inherent problems that are difficult to overcome. Oxidation presents the most significant problem, as it weakens the fiber and lowers the quality factor, severely limiting the theoretical advantages of using fused silica as suspension material. These problems were the incentive for researching amorphous metals as an alternative material for mirror suspensions. Amorphous MoRuB samples are currently being manufactured and tested for use as flex joints for mirror suspensions. Several material properties and sample characteristics have to be measured, in particular, it is necessary to certify each flex joint uniform, compact, and free from cracks both before and after manufacturing. Certifying that each joint is free from cracks down to a level substantially smaller than the material's catastrophic failure critical defect size (~100 μm for MoRuB) is equivalent to certifying that the sample will not crack unless it is exposed to stresses exceeding the material ultimate yield strength. Good joint certification allows us to fully use the material's strength. This certification is made through X-ray imaging of the samples (in our case we used a diagnostic medical X-ray unit courtesy of the Animal Care facility at Caltech), digitizing the images using a scanner (in our case a slide scanner courtesy of Caltech's Digital Media Center), and then analyzing the results. We developed a process that certifies a sample as being uniform (same thickness throughout and free of any holes/cracks) and therefore suitable for use as a flex-joint suspension. This certification process is also applied to all samples used to measure the material's properties.

1. Introduction

The purpose of LIGO (Laser Interferometer Gravitational-wave Observatory) is to detect gravity waves. Gravity waves are predicted through Einstein's theory of General Relativity. In this theory, the warping of space-time describes gravity. When a massive object is quickly accelerated, it causes a ripple in the fabric of space-time that propagates at the speed of light- a gravity wave. Gravity waves are expected to be produced by events such as neutron stars orbiting each other at small radii and ultimately coalescing into black holes, super nova explosions, or the big bang. By studying the gravity waves emitted by such events we can learn many things about features in our universe that are currently largely mysteries to us, black holes for example.

A Michelson Morley laser interferometer is being used to detect these gravity waves. This is a device in which a laser beam is split and sent down two perpendicular, vacuum-sealed arms of equal length (4km for LIGO). At the end of each arm hangs a mirror acting as a test mass. The mirror reflects the laser light back to the central station.

The interferometer is set up so that if the distance the light travels down the two arms is the same to a small fraction of a wavelength, in the absence of perturbations, the light interferes destructively and gives no signal. If the arms are perturbed, some light travels to a photo-detector and produces a signal. With this device, once the masses are sufficiently isolated from ground perturbations, we should be sensitive to the perturbations generated by the gravity waves, which will lengthen one arm and shorten the other.

In the search for gravity waves via laser interferometers, we will be constantly fighting a battle to reduce noise and identify weaker signals. There are many factors which limit the interferometer sensitivity- suspension thermal noise, mirror thermal noise, seismic noise, electrical noise, radiation pressure noise- only to mention a few. Most of the work being done on Advanced LIGO is on reducing the noise- therefore enhancing the ability to discern a gravitational wave amongst all the noise. With the development of improved seismic isolation systems, suspension thermal noise has become one of the limiting factors. Currently, the suspensions are essentially made out of piano wire slung around the mirror. The present assumption is that fused silica fibers are the ideal suspension for Advanced LIGO due to its theoretically high tensile strength and mechanical quality factor. However, there are problems that severely limit the theoretical strength and Q-factor values. The most significant problem is hydroxyl surface corrosion ($O + H_2O \rightarrow 2\ OH$), which, coupled with the very low fracture toughness of fused silica, weakens the fiber, limits its practical loading factor and lowers the quality factor, thereby limiting the theoretical advantages of using fused silica as suspension material. This has given birth to some research being done in possibly using amorphous metal flex joints as mirror suspensions. We believe that amorphous metal flex joints could give better performance because they have high tensile strength, corrosion resistance, and good Q-factor values. Also, the suspension effective quality factor can be enhanced mechanically due to the superior machine-ability of metal. Several glassy metals can be considered. Amorphous MoRuB has been chosen because of its strength, fracture toughness, corrosion resistance and low mechanical loss factor.[i]

Currently the shape of the flex joint being considered is about 300 μm long, 3mm wide, and 10 microns thick, machined from 5x3 mm, 50 μm thick platelets. Before hanging a mirror weighing a few tens of kilograms and costing a good fraction of a million-dollars off of a few sheets of 10-micron thick metal, we want to verify that the flex joint is correctly constructed and is not going to break. A series of procedures have been developed in order to ensure that our flex joint is suitable. These tests include, but are not limited too, X-ray diffraction measurements to ensure full glassiness, stress strain tests, and, the focus of this paper, X-ray micro-densitometry imaging.[ii] X-ray imaging is necessary for four main reasons:

- to determine the uniformity of the thickness, compactness, and density of the splat-quenched sample
- to certify the absence of cracks or holes (larger than the critical defect size) in the splat-quenched sample
- to select a region of the splat-quenched sample suitable to flex-joint creation
- to certify the final flex joint is uniform, has the desired shape, and is defect free

We developed the X-ray imaging process to perform these tasks. At present, X-ray imaging has already proved a useful tool for evaluating the success of the splatting process, and, together with the X-ray scattering measurement, assessing which regions of the sample are polluted by crystals and which are purely glassy.

2. Findings

The X-ray process developed consists of three main stages:

- X-ray imaging the sample
- digitizing the image
- analyzing the image in Matlab

This process was found to be effective for the four purposes it was created for.

Additional bonuses

Splat samples are mechanically and then electrochemically polished (a process that smoothes the surface, but when done in the presence of crystals it eats away the crystal leaving a hole). Samples that were partially crystalline presented holes that were clearly imaged in X-ray micro-densitometry. These holes can be clearly seen in figure 11- indicating that X-ray imaging is effective for locating both holes and cracks in the sample (complementing X-ray scattering in glassiness certification).

Samples just after splat quenching can be seen in figure 6, where we can clearly see that on three of the four splats, the surface shows a wedge shape. We also determined from these images that, in general, the thicker half of the wedge is brittle (partially crystalline), while the thinner part is generally amorphous. Studying this image illustrates how we were capable of determining several splat characteristics and providing feedback to the splat quenching process. In particular X-ray micro-densitometry made it clear that realigning the pistons for more level splats was necessary and guided the fine tuning of splat temperature and piston speed.

Technique limitations

We determined through some calculations regarding pixel size, source parallax etc... (see 4.9b) that the resolution of our scanning was limited by the scanner pixel size, which was six by six microns. This assures that the technique is capable to detect a defect down to that size. This is a sufficient resolution to certify glassy metals because the critical defect size is on the order of 100 microns for amorphous MoRuB[iii] (to be compared with fused silica, which has nanometer scale critical defect size). Our density resolution (what minimal thickness variation can be detected) is better than our transversal resolution, as we can resolve surface variations on the order of 27 microns over a large scale and 4.353 microns locally.[iv](See 4.8b, 4.92)

3. Conclusion

The development of the X-ray micro-densitometry technique was deemed a success, as we developed a process and determined it to be capable of doing three of its four designated tasks: determining uniformity, locating cracks or holes, and identifying amorphous regions. The fourth task, characterize the finished flex joint dimensions, is

expected to be a straightforward development. The resolution is already quite good. With more work on the setup the precision can be worked out more thoroughly and can be improved, as the techniques are refined. We do, however, already have a method for checking splat-quenched samples.

4. Method and the Development of the X-Ray process

4.1 Dental X-Rays initial measurements

At first, the feasibility of imaging our amorphous samples (MoRuB in these cases) with X-rays, and of resolving the image into valuable data, was not known. Prior to investing much money and time into the project, we set about to determine the feasibility. Since the process we had in mind involved three steps- X-raying the sample, digitizing the image, and analyzing the image in Matlab- we needed verification of each step's practicability. In order to X-ray our sample, we visited Dr. Russel Rose, a dentist in South Pasadena, who permitted us to use his dental X-ray unit (Belmont Equipment Corp. dental X-ray machine model: DX-807) and dental X-ray film (Kodak insight dental film) to make initial imaging of some MoRuB samples. On this unit we could adjust the power of the current hitting the W-tip of the X-ray unit as well as the time of exposure, therefore controlling the intensity of the X-ray beam. Using Dr. Rose's experience in guessing power and time settings, and eyeballing the film that was developed we could rapidly determine the variables and obtained an acceptable film. Through this trial and error method we found the optimal power and time values for this machine and this film (90Kv, 10mA, and .20s). We simply eyeballed that the film in the sample region was exposed to roughly half density. This indicated immediately that with closer quantitative film optical density analysis we would be able to determine thickness variations. We also could very clearly see the cracks in our sample, confirming that X-raying micro-densitometry was a very viable technique.

Was digitizing and quantitative analysis feasible? Courtesy of Virginio Sannibale's personal scanner, we were able to scan these dental X-rays in an 8-bit grayscale. These files were then saved as jpeg's and transported back on campus. These jpeg files were then imported into Matlab and the sample was imaged in a color-scale associated with the grayscale. This first measurement can be seen in figure 1. Just a glance at this image showed that we could determine homogeneity of the sample's thickness and the presence of cracks.

Figure 1

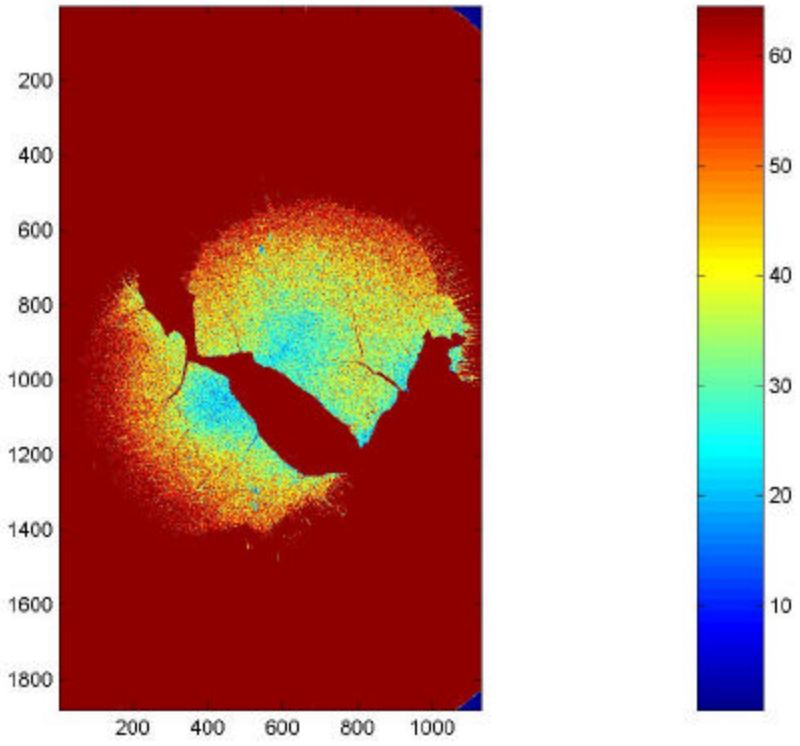

4.2 Dental X-ray Technique Problems and Limitations

The initial measurements showed that what we wanted to do was possible; we only needed to refine the technique. Every step of X-ray imaging could be improved upon. The first problem observed was with the X-ray unit. By focusing on the contrast in the background of the image in figure 1 we find figure 2.

Figure 2

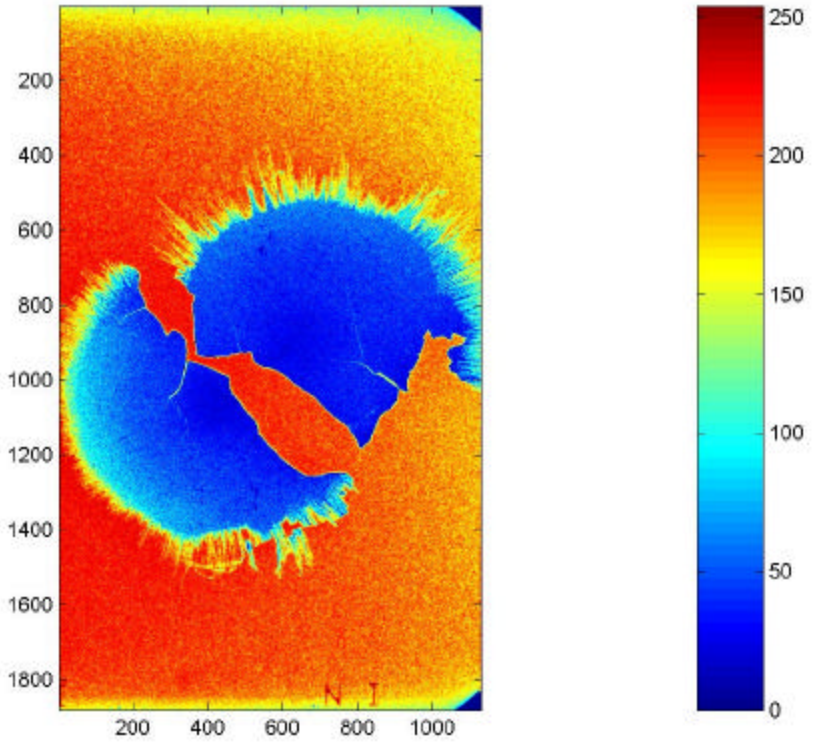

In this image, we clearly discern the exposure gradient and the halo from the dentist's X-ray gun collimator shade. The dental X-rays are collimated with a circular tube. We can see the density gradient starting from the edge of this tube in the circular shape in the two right corners of the image, increasing from orange-yellow to the red-orange more heavily exposed region close to the sample. The image taken was also simply taken on a dentist's chair, which is an uneven surface with underlying metal beams, which could cause uncontrolled reflections of the X-rays, making the exposure of the film inhomogeneous.

Second, the film used by dentists does not require the resolution that we desire. We contacted Kodak and spoke with Franklin Brayer, who works in film development. He indicated the Kodak Insight film we had used was optimized for quick exposure to reduce X-ray dosage to the patients, but was not designed for uniform, high sensitivity and high-resolution exposure.

A third problem lay with the scanning of the image. The image was scanned on an 8-bit grayscale, which limits the grayscale intensity number to 0-255, limiting the thickness resolution (small grayscale changes). We also made the mistake to save our scanned files in the jpeg format. This format compresses the files by eliminating higher order Fourier terms for easy transfer. This compressing process reduces the sharpness of our crack resolution and produces other artifacts. All of these mistakes and shortcoming were addressed in the following batches of images.

4.3 Improvements over Dental X-rays

The first thing that we needed to fix was the problem of inhomogeneity in the X-ray unit. Searching on campus, we found that the animal care facility has a diagnostic X-ray unit (the same used on people). This unit allows imaging over a large region, with more uniform exposure, and is fixed over a table perpendicular to its beam, which does not have the same reflection problems of a dental chair. This unit does not allow control over the time of exposure (it has an internal limit so people/animals are not overdosed) but allows much more control over the power and total exposure of the X-ray.

To fix the film problem we switched to mammography film, which is designed to be very sensitive to X-rays and should have resolution even on a finer scale than we are concerned with.

For the scanning problems we turned to the Digital Media Center on Caltech campus. At this facility, we are able to scan our X-rays in a 16-bit grayscale, enabling an optical density ranging from 0-65,535.

We then saved our data as tif files (a no-compression, no-loss format) and burned them to a CD for transport to a computer for Matlab analysis.

4.4 First Diagnostic Run (Run A)

Using the same trial and error technique employed at the dentist, we were able to find close to the optimal power settings for imaging our samples (MoRuB and metglass pieces in this instance). Since the film used was standard mammography film, our samples covered only a small portion of the film. In order to save time and expense, we took four exposures on one film, covering the regions we were not interested in with lead screens. We also collimated the X-ray beam to a quarter of the film. The films were then developed using the veterinary development machine. These developed images were then brought to the digital media center and scanned in a 16-bit grayscale at 800 ppi. Fine tuning of the exposure settings for the following runs were determined by viewing these images through the color-scale created by Matlab. The grayscale map ranging from zero to 65,535 improved our density resolution by a large factor. These new machines were much more capable and effective than the dental technique, as can be determined from figure 3. We also could tell from figure 3 that a stack of metglass 18 μm thick film would function well as a calibration scale.

Figure 3

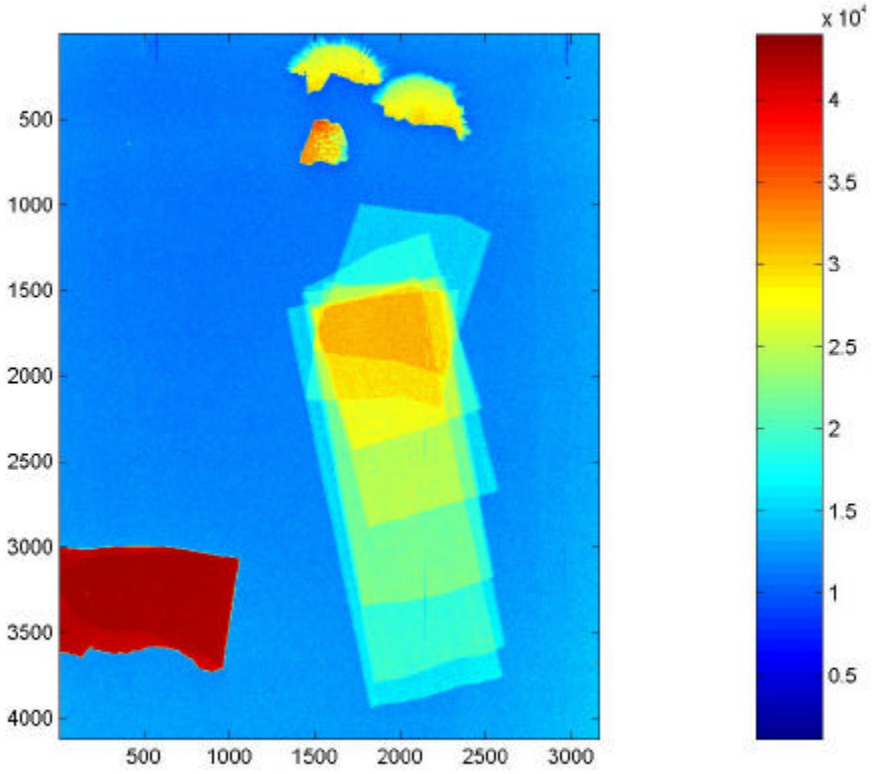

4.5 Problems with Diagnostic Run A and Improvements for Run B

Even though the first diagnostic run showed a marked improvement upon the dental run, it was far from perfect. We took multiple exposures on the same film, covering unused sections of the film with lead. Analysis showed some overexposed dots, probably due to places where holes in the lead shield had not blocked the X-rays. To do precise analysis and still take multiple exposures on one film we constructed our own uniform and more precisely shaped lead shield. We did this with a sheet of lead 5 millimeters thick. The sheet of lead was sandwiched between two sheets of aluminum for rigidity, and was supported by two bars of aluminum to hold the shield above the film case (when imaging the film it is contained inside an aluminum case to prevent exposure to ambient light, low energy rays, etc...). A rectangular window was cut in the lead and aluminum structure to allow for imaging, and a piece of Mylar film is affixed on the window to support the samples and the calibration scale for quick and easy shifting and imaging. The 20.5 x 5 cm rectangular window was chosen to allow for four separate strips to be imaged in succession with minimal motion of the film and the shield. One possible problem with this method is determining which part of the film has already been exposed. The solution to this problem is simply a large piece of paper with labels of which exposure each region is associated with (the effects of the paper and the Mylar are negligible and uniform on the X-ray fields).

The next factor that needed improvement was the calibration scale. The concept behind the calibration scale is relatively simple. A stack of strips of metglass created a

ladder one piece thick on one end and 15 on the other (seen as imaged in figure 5). By imaging this scale, and plotting the mean intensity number versus thickness of metglass, we get a curve that tells us what a certain intensity number is in terms of thickness in metglass layers. A sample curve can be seen in figure 4.

Figure 4

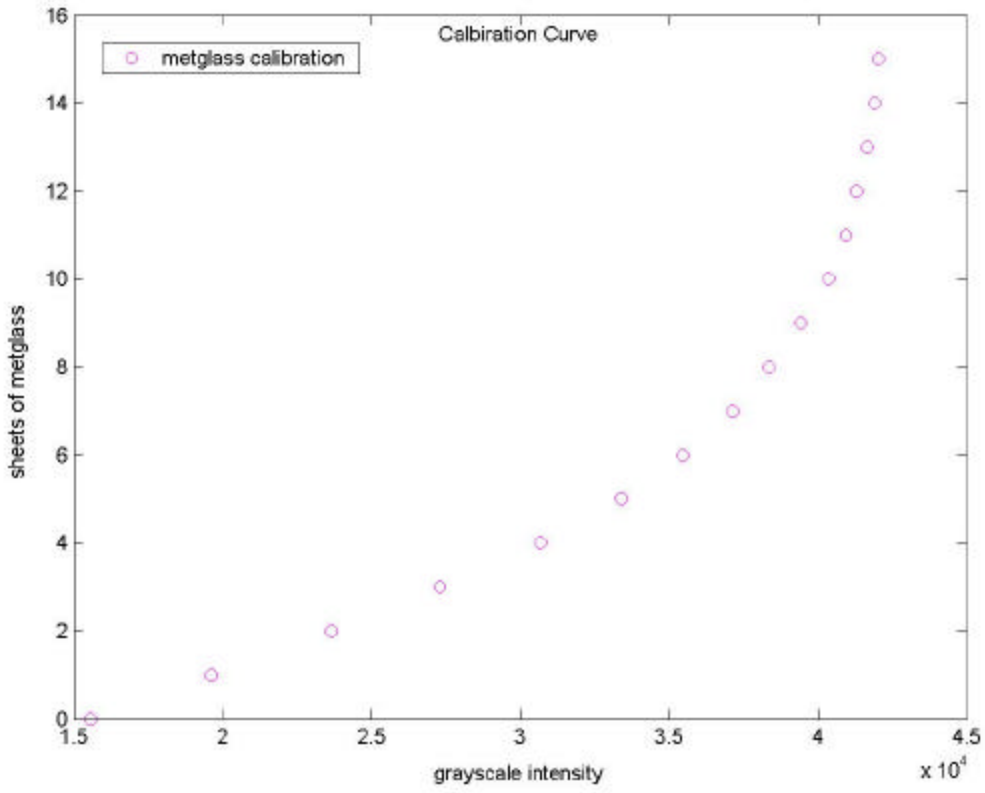

Then the multiplicative factor between sheets of metglass and microns of MoRuB can be determined by comparing with a piece of MoRuB of uniform and known thickness, thereby enabling us to use the measured shape of the metglass ladder calibration curve to generate a linearized thickness scale for MoRuB.

Figure 5

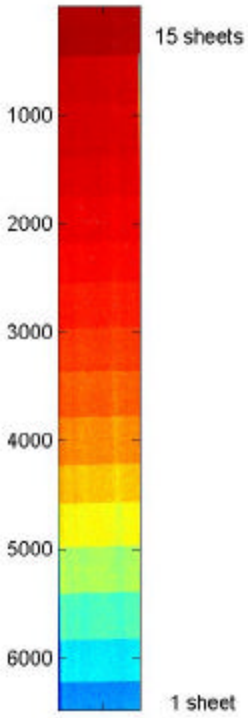

4.6 X-Ray Run B

With X-ray run B we were able to find the optimal setting for the X-ray unit based upon the knowledge gained from run A. The settings were as follows- X-ray gun 32 inches above the table, current set at 50Kv and 2.5mAs, and an exposure time of .024 seconds. By using our new shield we were able to take very good images of some samples, giving us some real feedback on the samples characteristics.

Figure 6

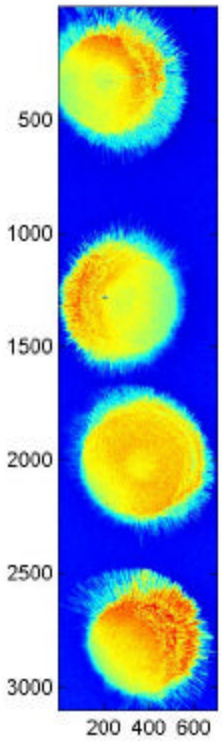

In Figure 6 one can see the characteristics of four samples. It is plain to see that most splats exhibit a wedge shaped trend supposedly due to imperfections in the creation process. The images also show the effects of different splatting parameters on the uniformity and size of the glassy portion at the center of the splat and will allow us to correlate the thickness with the glassiness of the resulting film. These are very interesting results, allowing us to quantify a problem in the creation process and provide feedback to fix it. Additionally, knowing the direction of the thickness gradient will allow us to choose from what portion of the splat and in which direction to cut the flex joints that we want to manufacture. This result also shows that the technique will be capable of certifying the thickness uniformity of our samples.

Figure 7

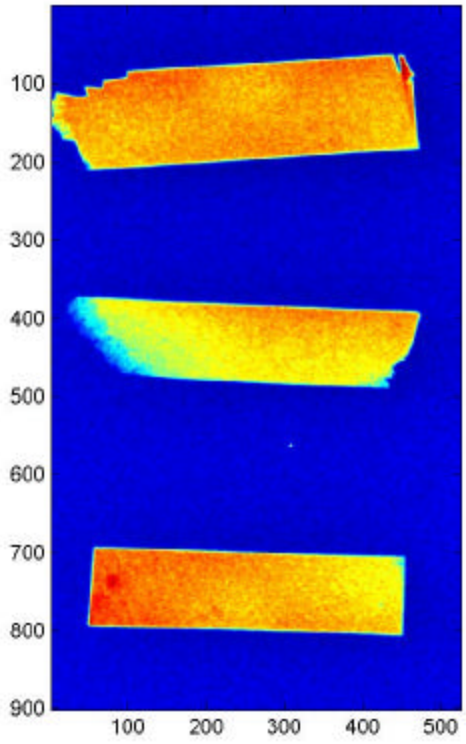

In figure 7 we can see strips that were EDM (electro-discharge machine) cut out of circular splats. The thickness trend is clearly visible in the second and third piece. However, by also imaging our samples with an optical microscope, we found that the X-ray could not pick up small surface features; an optical microscope is necessary in addition to the X-ray to certify surface homogeneity.

The learning curve (The reader less interested in the details of our naiveté is invited to skip to section 4.8b)

When it seemed that all that was left was calculations using the new calibration scale- a new problem arose. A careful analysis of the background intensity showed a gradient of the grayscale value incompatible with an equally exposed region. The background grayscale value changed gradually as a function of position- indicating that either the film sensitivity or the X-ray intensity was not uniform throughout the image. This meant that the calibration scale was not precise along the whole image.

In order to account for the gradient, we needed to know where the gradient came from. If it was due to inhomogeneity of the X-ray, it needed to be fixed by a multiplicative factor. If it was due to the film, an additive factor might be better to correct the problem.

4.7 X-ray Run C

In order to determine whether the inhomogeneity was due to the film or the X-ray, we took a blank exposure with the film orientated in one direction, and a second one with the film inverted. If the film was the source of the inhomogeneity, then the gradient

would be in the same direction with respect to the film, if the X-ray was the source of the inhomogeneity, than the gradient would be in opposite directions on the film (the same direction relative to the X-ray unit). At first appearance it seemed as though the X-ray unit was the source of the problems, as the gradient was in opposite directions with respect to the film.

We also wanted to see if the gradient was similar for samples of given thickness. Hence, when imaging the sample we placed strips of metglass, each four sheets thick, spaced throughout the region. By then subtracting the background gradient from the 4-sheet gradient we could determine whether the gradient was the same for our samples as the background region. It did turn out that the gradient was nearly the same in both cases, and the subtraction of the background gradient results in a nearly flat response. It was then concluded that if the calibration scale was corrected by dividing it by the background value near the sample, the effects of the gradient could be eliminated from the thickness calibration scale.

Since this method was not simple, we decided that for the next X-ray run we should try to eliminate the gradient source. Since the gradient seemed to be due to the X-ray field, we assumed that we could reduce it by opening the shutter of the X-rays wider. Since the shutters control the X-ray's beam dimensions, the shutters can interfere with the edges of the X-ray field, causing the intensity to fall off as one approaches the edges of the beam. By simply expanding the beam size this edge problem should diminish, preventing or reducing the gradient problem altogether.

An odd thing discovered in this X-ray run can be seen in figure 8.

Figure 8

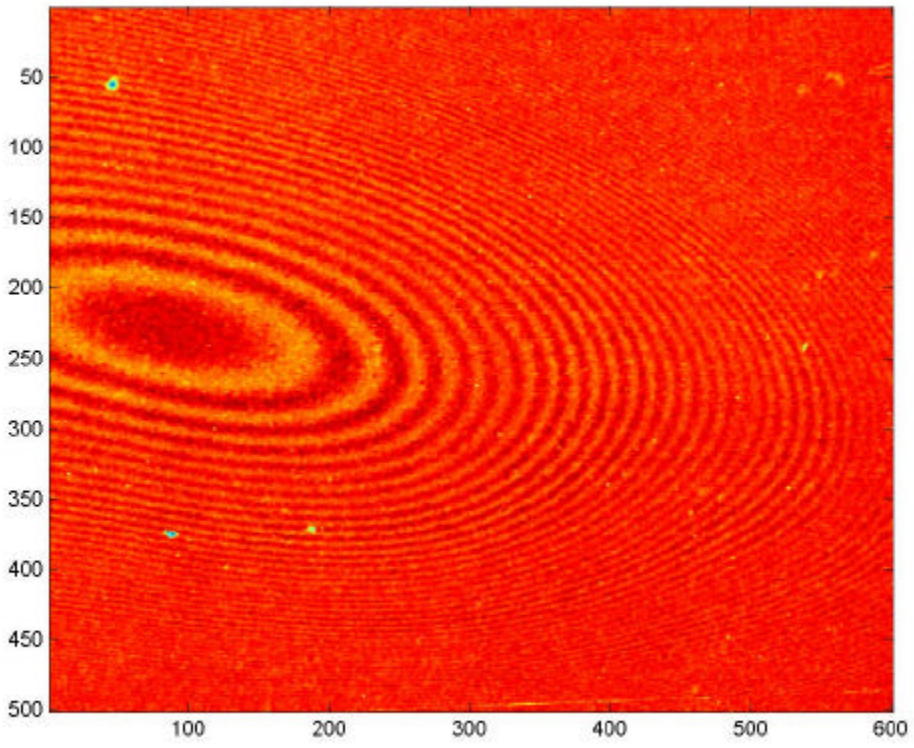

This image was found in a part of the MoRuB calibration sheet where it is about 14 sheets thick. Much confusion ensued about what this perfectly elliptically shaped thickness variation came from. It was decided that it probably was the ripples of an air bubble leaving the surface of the metglass during its spin casting. Since the metglass is so rapidly cooled what we see are the ripples frozen in time of the bubble escaping the surface. We found this discovery to be pleasing as it showed we are able to discern thickness fluctuations in thin films. It turned out later to be the wrong conclusion.

4.8 X-ray Run D

We started this X-ray session by opening the shutter so the X-ray target was about 2 inches wider than the lead mask on all sides of the imaged region. We hoped that the gradient was eliminated by this new technique. We also imaged some more samples, and repeated the exposure of some of the previously imaged samples with hopes of better calibrating the thickness. For all this the X-ray power settings remained at 50Kv, 2.5 mAs, and the exposure time remained at 0.024 seconds, and the same scanner equipment and settings were used.

4.8a Thickness/Gradient Data Analysis

Upon analysis of the results we found that the gradient had not gone away. What we noticed upon closer analysis was that the gradient was sharper in one blank image than the other, indicating that we were dealing with a combination of inhomogeneity of the film and the X-ray. With the film oriented in one direction, the two gradients almost cancelled out, but when oriented in the other way, the two gradients seemed to add. This discovery was discouraging as it would be very difficult to quantify both gradients, and then subtract them from our data.

We needed to try to account for the gradient without having to quantify each aspect of it. To do this we thought of X-raying the calibration scale, in two separate images, with the reverse orientation in each exposure, so that the gradient acts in opposite directions on the calibration scale. By averaging the value for each thickness from the two calibration scales, we would get a gradient-free calibration scale. However, we needed a method to relate our sample's intensity number to this calibration scale while eliminating the gradient. Since we had measured that the gradient was almost the same shape in the background as on the samples, we decided to simply subtract the background from the intensity number to eliminate the gradient effect. However, in order to maintain the best absolute calibration near the samples of interest, we multiplied the data by a local correction factor determined by local calibrators, each 8 layers thick- the same as the central step of the calibration ladder.

Since on this X-ray run we had imaged the calibration scale in different orientations, we had all the data needed for this technique. The technique seemed to be working very well, we crosschecked measuring the thickness of a calibration piece 6 sheets thick and got results within 2.5% precision while being generous with the error bars. The calibration, so far obtained for metglass thickness, was converted into MoRuB thickness by relating the grayscale number of the measurement of a piece of MoRuB we had measured to be 53 microns thick with that of the calibration scale. Unfortunately, we then found inconsistencies in other data that substantially degraded our confidence in our absolute calibration. The disappointing discovery that this technique did not work well

was attributed to the quality of the gradient being due to both the X-ray and the film. This technique could eliminate a gradient introduced by a multiplicative factor (X-ray gradient), but not a gradient introduced by an additive factor (film gradient). So the seemingly good initial result we had were really an illusion, and a new approach was needed.

At this point, since the observed gradients was always quite slow and smooth, we abandoned the idea of making an absolute calibration of a large field of view and we resorted to a local linearization of the scale near each sample. This way the error is reduced to the gradient integrated over a smaller region. The way we planned to apply this technique was to place two metglass calibration pieces by each sample (one 4 sheets, and the other 7 sheets thick to bracket the 'X-ray thickness' of our samples), and use these values for the local linearization.

4.8b Gaussian fit analysis of the samples optical density

In order to determine the sample's thickness uniformity we applied a Gaussian fit analysis. We plot a histogram of the grayscale number in selected regions: the background, pieces of metglass, and pieces of MoRuB. By doing a Gaussian fit of these histograms (on Kaleidograph) we can see whether the spread of our data is actually Gaussian. The measurement's resolution is determined by the width of the Gaussians of data taken on the background and on guaranteed flat test pieces. The width of the background Gaussian determines the limitation of the method- no matter how perfect our sample is the Gaussian of the sample must be at least as wide of that of the background. Since there are actually less photons penetrating our sample and interacting on the film, our samples Gaussian will almost certainly be wider. This would lead one to think that the Gaussian of a piece of metglass of comparable thickness might be our limiting width- but the inhomogeneity of the metglass surface can even be larger than that on our samples. Therefore, by quadratically subtracting the background's standard deviation from our samples standard deviation we find the upper limit of the value for the variations in thickness of our sample. If we image a piece of MoRuB, and its standard deviation is equal to that of the background, it means the piece is perfect as far as we can tell. However, since there is an evaluation error in the standard deviation, this error will determine the actual surface fluctuations that might still be there beyond our resolution. The formula calculating the standard deviation evaluation error is just our standard deviation divided by the square root of the number of elements in the histogram. This approach seemed promising and could be used effectively once the gradient/calibration problem was fixed.

4.9 X-Ray Run E

For this X-ray session we added to the calibration ladder local calibration pieces, four and seven metglass sheets thick, next to every sample. As a crosscheck we replaced the samples by stacks of Metglass, each 6 sheet thick. By using the local linearization technique and comparing how close we get to six sheets, we can evaluate how good our system is. With our simple linearization, we found values of 6.10, 6.12, 6.15, and 6.15 sheets thick. It is not surprising that we are overestimating the value as we are idealizing a curve with a straight line. By being generous with our error bars and saying that we found our test piece within $\pm$ .2 sheets, we find an absolute error of 3.33%. This error is

acceptable to make flex joints, as the actual thickness value is not as crucial as the local thickness fluctuations. In addition, the actual thickness is already limited by our knowledge of our calibration piece of MoRuB that, being measured with a simple micrometer, has an error itself of at least 2%.

4.9a Ripple/Developing Problem

Once satisfied with our calibration technique we started to correlate grayscale thickness in term of microns of MoRuB. We once again decided to use the cut strip of MoRuB calculated to be 53 microns thick. However another problem was found.

Figure 9

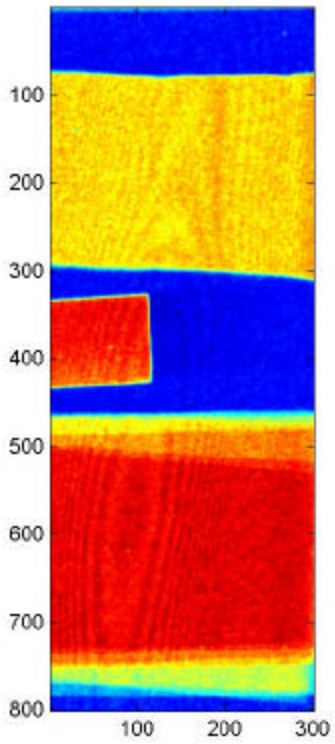

Illustrated in figure 9 is an object that appears to be similar to the ripple we found in the metglass and thought was the result of a bubble in the original melt. However, these ripples extend also into the background and into the piece of MoRuB- clearly this shape was not inside the metglass, it was either a product of the film or the scanner.

To test whether this error was introduced by the film or by the scanner, we began experimenting with the scanner. We scanned the same X-ray film again. We then simply lifted the top of the scanner and closed it again, and scanned again. We also took out the film and replaced it, and scanned it once more. By going through this process we were hoping to see whether the same shape appeared in the same region of the scanner or of the film. We also tested the importance of cleanliness in imaging, by scanning, putting a thumbprint on the scanner, and scanning again.

We found a couple of interesting things.

Figure 10

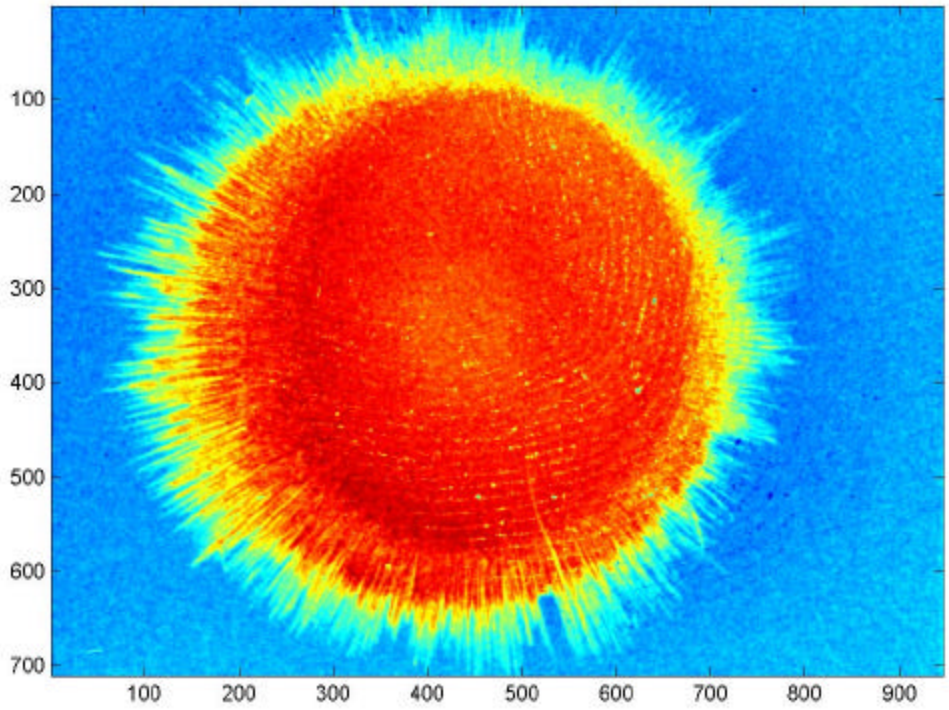

In figure 10 we can see the thumb print directly on top of the sample- evidence to us that we must be sure to keep things clean. We also found that the ripple shapes move around with relation to both the scanner and the film. This made us suspicious that the shapes were due to interaction between the scanner glass and the film, possibly interference patterns due to optical contact between the film and the glass of the scanner. To test this hypothesis we cut the film into strips that fit into plastic holder designed to hold negatives off the glass surface in the scanner. Repeated imaging with this technique confirmed the hypothesis- we found no ripples of any shape or form in any location with this technique.

One other small source of error that we noticed in this time of close analysis was that the film is not perfect. In its development process sometimes spots and scratches are left on the film. In order to correct for this problem we will image all of our samples on two different exposures, and then compare them. If an apparent hole/crack appears in only one image, we know it was the film, but if it is in the same place in two images, we know it is a defect in the object. With this simple technique, we can eliminate the development problem.

4.9b Determination of Pixel Size

We now had satisfactory control of the system calibration and knowledge of many sources of error and performance degradation. We began to determine the spatial resolution limitations of our system. The first thing we were interested in was the effective size of our pixels, a factor that limited our sensitivity to thickness variations over small distances. We used two different approaches to calculate this value. The first

approach was a direct determination based on the resolution of the scan. We scanned our image at 800 ppi.[v] Therefore, by simply converting this value to metric units and finding the inverse we can find our physical pixel size. With 800 ppi scanning, the length of each pixel edge turns out to be about 30 microns (31.75 microns).

To check this number and confirm we scanned at the resolution desired we used our calibration sample of MoRuB again. Since it had been cut into a nearly perfect rectangle, we knew its length and width precisely. By finding its pixel length and width we could calculate the pixel size. These calculations confirmed the 30 microns per pixel calculated before. However, this resolution is not completely satisfactory. If each pixel was 30 microns in size, a dent on the order of ten microns probably will not be apparent in the data. This is a worrisome limitation if we want to guarantee that the final flex joint is free of cracks of critical size (~100 μm), and one that we need to fix. The simple solution was to turn to a higher resolution scanner. Up until this time we had been using a standard scanning unit, but by cutting up our X-ray films, we could insert them in a slide-scanning unit that had the capability to scan at 4000 ppi- a large enough improvement upon 800 ppi. We had not turned to this before because we would not have been able to scan our calibration scale. However, with our new local linearization technique, we only need to scan a small region at once.

By testing using the same images from run F we confirmed that the slide scanner was a feasible option, as it worked- there were no ripples present in the scanned images. We checked the pixel size of the 4000 ppi scanner and confirmed that the pixels were now six by six microns. It now appeared as though we had a technique that would work from start to finish. It only really remained for us to determine two more factors before the system could begin to really certify samples. We needed to determine our limit of thickness measurements- what size thickness fluctuation we could not see. We also needed to confirm that holes would be visible through this imaging technique.

4.91 X-Ray Run F

For this imaging session we had a new procedure that we employed with confidence. We no longer needed and therefore no longer used the full calibration scale- we simply used the local linearization technique for every sample. We made sure to bracket the MoRuB calibration piece with known thickness, as well as some cut strips. The majority of what we imaged were pieces that had been electrochemically polished. This is a process which we will use to make the surface of samples smooth, as well as a method of thinning our samples from ~50 microns down to ~10 microns thick in the actual flex joint region. One of the advantages of this technique is that if there are any crystals present in the glass, they will be 'eaten away' preferentially, leaving holes behind. This is good because if we can see any hole, we can immediately see that the sample is a bad sample and reject it. It is much easier to see a hole than whether a material is in a crystalline or amorphous phase. By imaging samples that had been electro-polished we hoped to confirm that we could locate the holes left by the crystals. For this measurement we chose the edge of a splat where the cooling is deficient and we know that crystals must be present.

Aside from the changes with the calibration scale, double exposures, and the scanner used- everything else remained the same, X-ray power, height, etc… The results we got were pleasing.

Figure 11

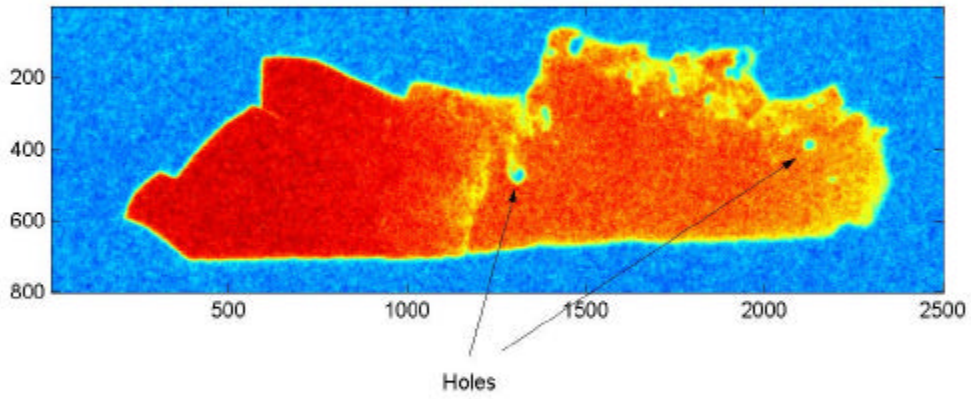

In figure 11 one can clearly see the holes remaining from electrochemical polishing. This confirmed our capability to detect holes.

4.92 Final considerations

We earlier spoke of the pixels being six microns by six microns, but we had to determine whether the pixel size was the limiting factor, or the film grain size. With the assistance of Professor Francesco Fidecaro we looked at some background region of an image. Using a technique consisting of a 2-D fast-fourier transform followed by a 2-D correlation function in Matlab, we determined there was no relationship between a pixel and the neighboring pixels, indicating that the film grain is smaller than the pixel size, and the pixels are the limiting factor.

Concurrently, we also worked on a 2-D profiling technique in Matlab, to supplement the color maps. By taking slices of a sample (generally ~10 pixels wide), averaging each part of the slice (width-wise), and then plotting these average points on a graph we can study general surface trends. As expected, it shows a smoother profile that has reduced random error due to the averaging (also implying lower resolution).

The last point left to evaluate is the smallest thickness fluctuation that can be distinguished. Using the technique discussed in the Gaussian fit section, we determined the optical thickness variance. Each pixel integrates the optical density over the pixel area (say 6 by 6 microns) and we can detect a defect only if it generates an optical thickness variation larger than the local optical thickness variance. This is function of the

sample rugosity as well as of the method limitations. A variation of several percent over a single pixel is a detectable defect. Also it should be noted that the technique is incapable to distinguish between a thickness variation over the entire pixel and, for example, a minute through hole taking away the same amount of matter from the volume covered by the pixel. Fortunately, these kinds of defects are not possible in glassy materials. The important point to be stressed is that this technique is sensitive to defects much smaller than the Glassy metal critical defect size, and that any defect small enough not to be detectable by this technique will not degrade in any way the performance and reliability of the inspected flex joint. We found that we could resolve surface variations on the order of 4.343 microns locally and 27 microns overall.

5. Acknowledgements

I would like to thank Dr. Riccardo DeSalvo for his unending assistance. Hareem Tariq for her patience and helpful advice. The Animal Care facility for their generosity and aid. The Digital Media Center for their help. Dr. Russel Rose for his assistance. Professor Johnson and Dr. Jan Schroer for their help with making and understanding amorphous metals. Stoyan Nikolov for his quick understanding and assistance that propelled the project forwards. Professor Francesco Fidecaro, Virginio Sannibale, Mike Hall, Yoichi Aso, Kelin Wang, Brian Emmerson, Stefano Tirelli, and the rest of the students in Riccardo's group for their assistance and advice. I would also like the thank Caltech, LIGO, the LIGO REU program, and the SURF office for the opportunity. Finally, it is necessary for me to thank the animals that waited patiently for the X-ray machine.

[i] For more information on glassy metals versus fused silica see:
DeSalvo, Riccardo (2002). Are Glassy Metal flex joints better than fused silica fibers for mirror suspensions? Presentation, LIGO document LIGO-G020445-00-R

[ii] For more information on other certification tests and material properties see:
Simoni, Barbara (2002). SURF final presentation, Phase transition heat in MoRuB. Presentation, LIGO document LIGO-G020439-00-R

Mantovani, Maddelena (2002). SURF final presentation, Hardness and Elasticity Measurements in MoRuB. Presentation, LIGO document LIGO-G020440-00-R

Tirelli, Stefano (2002). SURF final presentation, Stress-strain behavior of MoRuB glassy metals. Presentation, LIGO document LIGO-G020441-00-R

Hall, Michael (2002). SURF final presentation, Physical Property Measurements of Glassy Metals. Presentation, LIGO document LIGO-G020443-00-R

Emmerson, Brian (2002). X-ray scattering measurements of crystallite contamination in glassy metals (updated). Presentation, LIGO document LIGO-G-020444-00-R

Papers on each presentation forthcoming

[iii] Professor Johnson's estimate

[iv] Calculation done by Stoyan Nikolov

[v] It had appeared all along that we were scanning at a resolution of 800 dpi, however, the computer indicated that we were using dpi, but after further research into scanners with the assistance of the Digital Media Center it was determined that dpi (dot per inch) was a misnomer in this instance, as the scanner actually was scanning at 800 ppi (pixels per inch). It turns out that there is much confusion about these two terms, and that dpi is only used for printers, as they print with dots, and that ppi is the unit of measure used with a scanner.

References

1) DeSalvo, Riccardo (2002). Are Glassy Metal flex joints better than fused silica fibers for mirror suspensions? Presentation, LIGO document LIGO-G020445-00-R

2) Simoni, Barbara (2002). SURF final presentation, Phase transition heat in MoRuB. Presentation, LIGO document LIGO-G020439-00-R

3) Mantovani, Maddelena (2002). SURF final presentation, Hardness and Elasticity Measurements in MoRuB. Presentation, LIGO document LIGO-G020440-00-R

4) Tirelli, Stefano (2002). SURF final presentation, Stress-strain behavior of MoRuB glassy metals. Presentation, LIGO document LIGO-G020441-00-R

5) Hall, Michael (2002). SURF final presentation, Physical Property Measurements of Glassy Metals. Presentation, LIGO document LIGO-G020443-00-R

6) Emmerson, Brian (2002). X-ray scattering measurements of crystallite contamination in glassy metals (updated). Presentation, LIGO document LIGO-G-020444-00-R